CALCULATED AND MEASURED MAGNETIC FIELDS FOR THE INJECTOR CYCLOTRON AT THE NAC

Z.B. du Toit, L.M. Roels, H.N. Jungwirth, A.H. Botha
National Accelerator Centre, CSIR, P.O. Box 72 FAURE, 7131, REPUBLIC OF SOUTH AFRICA

Summary

A four-sector magnet, employing seven trim-coils and two sets of harmonic coils, has been designed by using a computer program developed in-house for calculation of three-dimensional magnetic fields. The program has been applied to determine the size and profile of the magnet poles and sectors. Results of subsequent field measurements will be presented in comparison with the calculated fields. The method by which isochronized fields are being generated and interpolated as well as the final shimming of the magnet will be discussed.

1. Introduction

The calculations for the design of the four-sector magnet of the injector cyclotron SPC1 were performed with a computer program POFEL3[1] developed at the NAC. POFEL3 solves the Laplace equation for a scalar potential $P(r,\theta,z)$ for Dirichlet boundary conditions imposed directly at nodes of a cylindrical co-ordinate grid. The whole magnet is first enclosed in a large cylindrical volume and, using a zooming technique, this is then systematically reduced to the required region with a much greater density of points. The solution is obtained in terms of the potential values $P(\ell,m,n)$ from which the magnetic field in the median plane can be derived. Unfortunately this formalism does not take saturation effects in account, but as our excitation range is very low we were fairly confident that deviations caused by saturation would be small, as the measured fields later proved.

The aim of our calculations was to determine the correct profile of the magnet pole tips, shims and centre disc to provide both an axially focusing field and an average magnetic field which could be isochronized for all particles and energies with the aid of 5 trim-coils, while keeping currents in these coils to a minimum. Another important consideration was that no particle should traverse the $\nu_r=1$ resonance before extraction.

Magnetic fields in the median plane were calculated for various pole geometries. On these main fields computed trim-coil fields were superimposed using a least-square approximation method, to make the field as isochronous as possible for the relevant particle and energy. Orbit calculations were then carried out in each computer-simulated field to investigate the focusing forces in the central region and during acceleration. Extraction through the fringe fields was also studied. These results allowed us to select a suitable configuration of the magnet poles and sectors, and led to the final dimensions of the magnet which are shown in figure 1.

2. Main field calculations

More than 30 main magnetic fields were calculated to optimize the pole profile. One of the more important and interesting features that came to light was the effect of the radial positioning of the magnet sectors. By moving the sectors 6 cm radially outwards ν_z-values

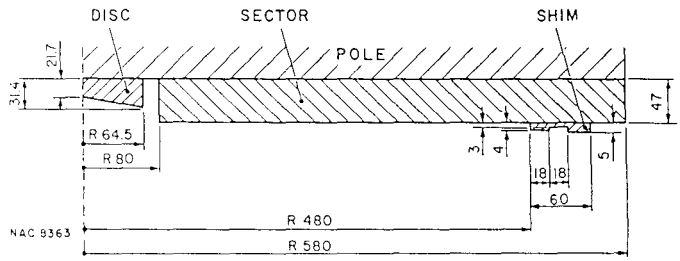

Fig. 1 Final dimensions of the pole sectors, centre disc and sector shims of SPC1.

were increased up to 50% in the central region, machining cost were reduced and more space was made available in the valleys. This allowed us to increase the azimuthal length of the harmonic coils, thus making them more effective.

Owing to the relatively large pole gap, the average magnetic field was found to fall too quickly near the edges of the poles. To correct this we decided to mount shims on the sector edges near the extraction radius. In order to obtain as much information as possible about the influence of such shims on the magnetic field, different shapes of varying radial length, radial position and thickness were represented in the computations. Figure 2 shows the increase of the average magnetic field for three different shims. Shim A has a radial length of 5 cm, extending from 49 cm to 54 cm and is 5 mm thick. Shim B has the same thickness, but extends from 50 cm to 55 cm. Shim C lies between radii 49 and 55 cm, with a thickness of 2.5 mm for the first 3 cm and a thickness of 5 mm for the remaining part.

Owing to the fact that the four magnet sectors are displaced radially outwards, the average magnetic field

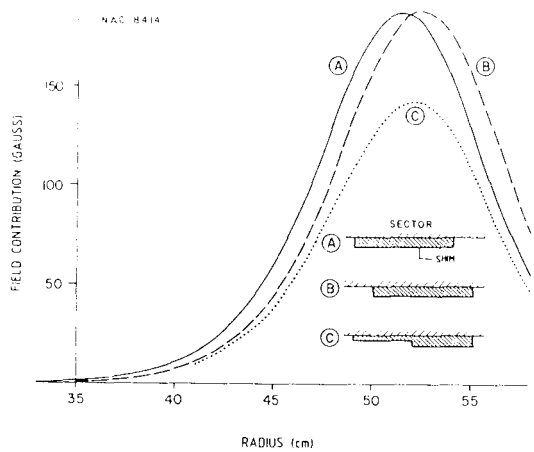

Fig. 2 Field contribution for different sector-shims. (See text).

CH1996-3/84/0000-094 $1.00 © 1984 IEEE

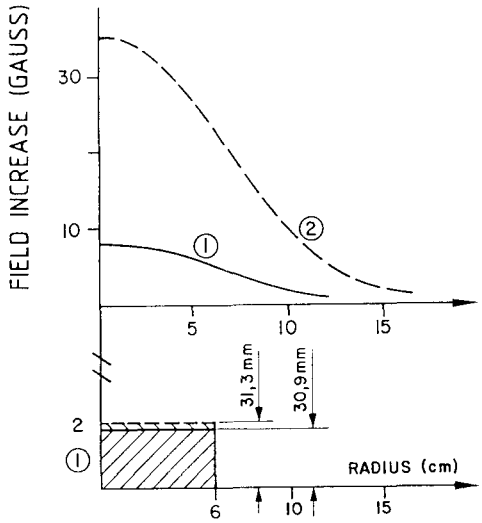

Fig. 3 Field increase due to two different centre discs. (See text).

as calculated with the POFEL3 program showed a dip in the central region. To fill up that dip, computations were carried out for discs of various profiles mounted in the centre of the machine. The influence of small changes to the geometry was also investigated. Figure 3 shows the increase in the average magnetic field caused by increasing the height of a 12 cm diameter centre disc. Curve 1 gives the increase of the average field resulting from increasing the height of the disc by 0.1 mm (from 30.8 to 30.9 mm) and curve 2 the result of increasing the height by 0.5 mm (from 30.8 to 31.3 mm).

3. Field calculations for the pole-gap coils

The pole-gap coils consist of 2 cone- and 5 trim-coils pairs and two sets of harmonic coils. Computer codes TRIMCO[2] and HARMCO[3] were developed specifically for the calculation of the axial component of the magnetic field in the median plane of the injector cyclotron due to the circular trim-coils and harmonic coils respectively. Both codes employ the method of mirror images in the calculation of the magnetic field. The calculations are minimised by making use of the symmetry properties of the coils. Each cone- and trim-coil consists of 3 turns of 5 mm square copper tubing with a 3 mm diameter cooling duct, while each harmonic coil consists of 10 windings of 4 x 2 mm copper conductor mounted onto a water-cooled plate. All coils are vacuum-cast epoxy impregnated. The two cone coils are situated at radii of 8 and 10 cm respectively, and the trim-coils at radii of 14, 18, 24, 34 and 47 cm respectively.

Two sets of harmonic coils, respectively situated at radii of approximately 18 and 48 cm were specified for the injector cyclotron. The inner set is intended for centring of the particle orbits while the outer set could either be used as a beam steering device or to assist the extraction process by the introduction of a suitable 1st-harmonic component in the main field.

Owing to the shape of a harmonic coil, the calculation of the z-component of its magnetic field in the median plane (i.e. $B_z(r,\theta,z=o)$) is more complicated than those for tne trim-coils. The field due to a harmonic coil and its mirror images was calculated in the following way: The contribution of each of the two radial segments of the coil (or coil image) is given by

$$B_z = -\frac{\mu_o . I}{4\pi}\int_{a_1}^{a_2} \frac{[\rho.\sin(\phi-\theta)].da}{[a^2+\rho^2+z^2-2a\rho.\cos(\phi-\theta)]^{3/2}}$$

where $\phi = \phi_1$ or ϕ_2 and $(\phi_2 - \phi_1)$ is the azimuthal extent of the coil. Parameters a_1 and a_2 are the radial boundaries of the circular segments of the coil.

The contribution of the two circular segments of the coil (i.e. arcs) is given by

$$B_z = -\frac{\mu_o . I . a}{4\pi}\int_{\phi_1}^{\phi_2} \frac{[\rho.\cos(\phi-\theta)-a].d\phi}{[a^2+\rho^2+z^2-2a\rho.\cos(\phi-\theta)]^{3/2}}$$

where $a = a_1$ or a_2 respectively for each circular segment and ϕ_1 and ϕ_2 are the azimuthal boundaries.

4. Field mapping equipment

A single InAs Hall-probe, with a temperature coefficient of about $3 \times 10^{-5}/^{o}C$, was mounted on a non-magnetic carriage and moved along a radial beam by a stepping motor and a cable system. A total distance of 60 cm could be covered in the radial direction and the beam could be extended telescopically to allow field measurement in the extraction region. This beam was mounted on a 1860 mm diameter aluminium ring gear with teeth at 3^{o} azimuthal increments. Rotation was accomplished by a pair of pneumatic cylinders and the final positioning was realised by locking the beam in place with a pneumatically driven roller wedge. The Hall-probe itself was mounted in a small aluminium oven in which the temperature could be kept constant with the aid of thermistors and a small control device. The heating of the oven was achieved by using two miniature strain-gauges as resistive elements of 120Ω each and the whole oven was heat-insulated by means of a bakelite case. With this arrangement the temperature of the Hall-probe could be kept at $27^{o}C$ with an accuracy of $0.1^{o}C$. Figure 4 shows the magnetic field measuring device with the aluminium ring gear and the telescopic beam on which the carriage is mounted.

The sheer mass of data required for a field map makes computerised data acquisition imperative. The field mapping equipment was therefore controlled from a minicomputer system by using the CAMAC instrumentation bus as a carrier for control commands and data. The data was pre-processed by translating voltage and position data to field and radius values according to a given algorithm and coefficients entered by the operator, and then transferred to a file. The control and acquisition program was written in-house owing to the interfacing necessary between the instruments and the minicomputer. It consists of a main routine which uses a menu driven display to allow non-technical/computer-knowledgeable operators to control the mapping procedure.

High precision voltmeters were used to measure outputs from Hall-probes and were interfaced to an IEEE-488 (General Purpose Instrumentation Bus GPIB) module resident in a CAMAC crate which was connected to the minicomputer on a CAMAC parallel branch cable approximately 600 metres away. The Hall-probe was positioned by stepper motors controlled via CAMAC stepper motor control modules from the minicomputer.

The computer-controlled measuring equipment operated smoothly and a typical field map consisting of 7200 points could be measured in 3½ hours. Such a map contains the field values at 120 azimuthal intervals of 3 degrees and at 60 radial intervals of 10 mm.

5. Comparison of calculated and measured fields

The main field (with current through the main coils only) was measured for various excitation currents (from 200 A to 800 A in steps of 50 A). In figure 5 the average magnetic field, normalised to unity in the centre of the machine, is shown as a function of the

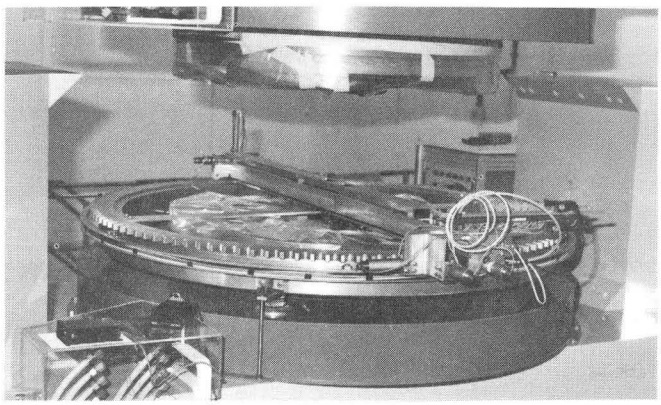

Fig. 4 The magnetic field measuring equipment in position in the pole gap of the light-ion injector cyclotron.

radius for excitation currents of 200 A, 450 A and 700 A. After this the magnetic field maps for each of the 5 pairs of trim-coils, 2 pairs of cone coils and the two sets of harmonic coils were measured at three different excitation levels in three different main fields. These measurements were only taken over a 90 degree azimuthal range as the main field measurements showed that deviations from four-fold symmetry were less than 0.02%.

One of the first fields we measured enabled us to check the accuracy of the computed magnetic fields. Apart from small differences due to the cylindrical grid approximation in the computer representation, the same geometry was used in the measured and the calculated fields. The centre discs were 30.8 mm high and 12 cm in diameter and the sector shims extended radially from 48 cm to 54 cm and were 5 mm high. An excitation current of 600 Amp was used and a complete field map was measured (from 0^{o} to 360^{o} in steps of 3^{o} and from 0 to 60 cm radius in 2 cm steps.) This measurement showed that the difference between the computed average field and measured average field along a radial line was less than 0.2% over the whole map up to the extraction radius. Near the edges of the poles the computed field was $\lesssim$ 1% higher than the measured one. This difference arises because the computer code does not take saturation into account. Figure 6 shows the field deviation (i.e. measured field minus simulated field) at two different radii, while figure 7 shows the deviation between the two average fields.

Agreement between the measured and calculated fields for the pole-gap coils was very good. Figure 8a shows the measured and computed average field values for trim-

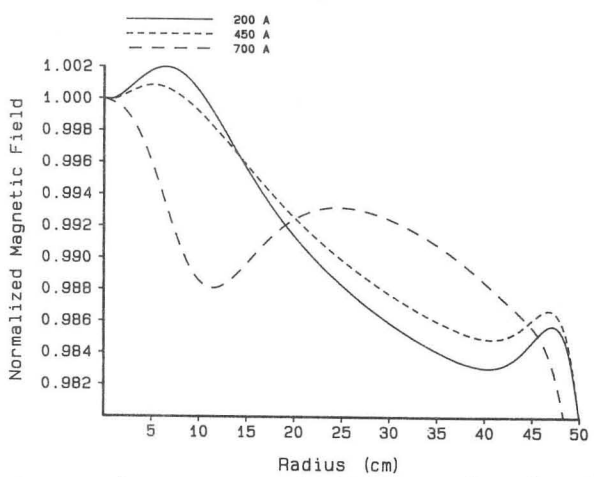

Fig. 5 Normalized average main field as a function of radius for excitation currents of 200A, 450A and 700A.

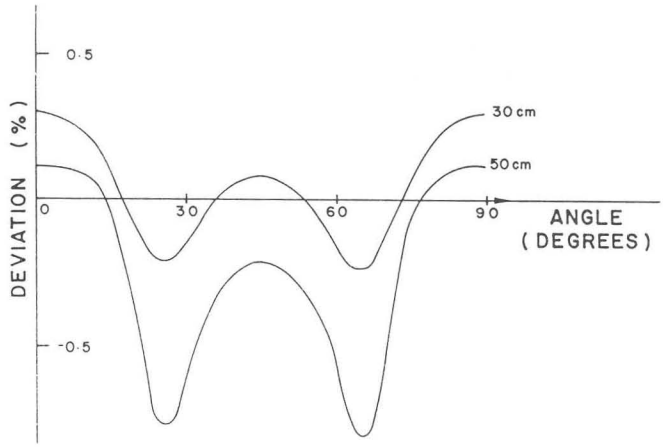

Fig. 6 Difference between calculated and measured fields over one sector at two different radii.

coil No. 5. In the pre-extraction region the computed values are within 3% of the measured values. In figure 8b & c the radial and azimuthal field distributions for a harmonic coil are shown. The full width at half maximum (FWHM) of the calculated azimuthal distribution is larger than the FWHM of the measured distribution by about 6% while the peak of the radial distribution is shifted by about 1 cm. These differences are, however, so small that no significant effect was seen in our orbit calculations.

All the measured trim-coil fields and main fields were then used in a calculation to determine the excitation currents required through the various coils for different specified field shapes. For this an algorithm was used for finding a set of trim-coil currents I_j, for j=1,..., n which for a given main field excitation H, will yield a resultant field that approximates a required field B as closely as possible.

We defined a sum of squares of differences between required and obtained field values as

$$S = \sum_{i=1}^{N} w_i \left[B_i - H_i - \sum_{j=1}^{n} T_i^j(I_j) \right]^2$$

where the subscript i defines the field point. The quantity $T^j(I_j)$ is the field due to the trim-coil current I_j, and w_i is a weighing factor.

The assumptions made were that the trim-coil currents were independent and that the fields were approxi-

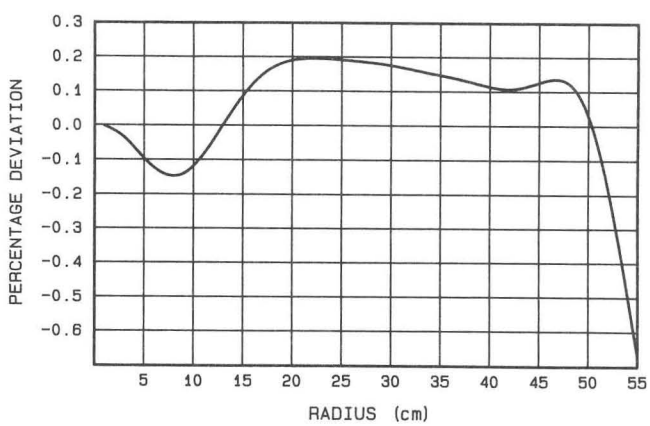

Fig. 7 Difference between calculated and measured average fields.

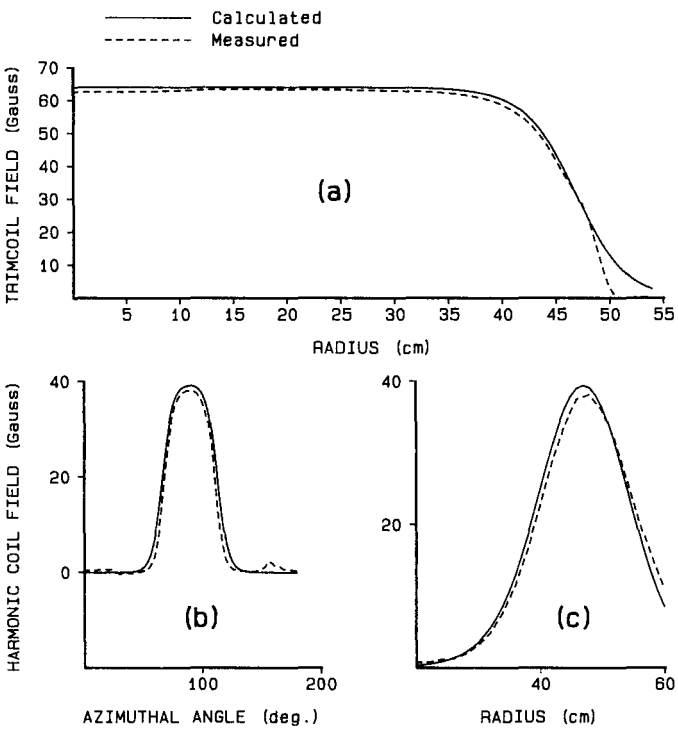

Fig. 8 Comparison of the calculated and measured values of the axial component of the magnetic flux density of a trim coil (a), and harmonic coil, (b) and (c).

mately linear functions of the excitation currents. Defining the trim-coil currents I_{jo} as the current values that minimise the sum of squares, S, we obtain a matrix equation.

$$\sum_{k=1}^{n} A_{jk} (I_{ko} - I_k) = B_j \quad \text{for } j = 1...., n$$

where

$$A_{jk} = \sum_{i=1}^{N} w_i \frac{\partial T_i^j(I_j)}{\partial I_j} \frac{\partial T_k^k(I_k)}{\partial I_k}$$

and

$$B_j = \sum_{i=1}^{N} w_i \left[B_i - H_i - \sum_{k=1}^{n} T_i^k(I_k) \right] \frac{\partial T_i^j(I_j)}{\partial I_j}$$

The matrix equation can be inverted to obtain a solution for I_{ko} in terms of a given value I_k. The algorithm as described was then programmed on the computer and it is possible now to get the required excitation currents for all the coils for any particle and energy in a few seconds.

As a final test, isochronous 8 MeV and 4 MeV proton fields were constructed with the results of this program and making use of the measured field maps. The 5 trim-coils were then excited to the calculated levels and a complete field map measured for comparison.

Figure 9 shows a typical result, the required average isochronous field, the constructed isochronous field, and the measured average field when all the coils are energised to the calculated values. As can be seen excellent agreement was obtained between the specified and measured field values. The deviation from the required average isochronous fields at radii up to 10 cm

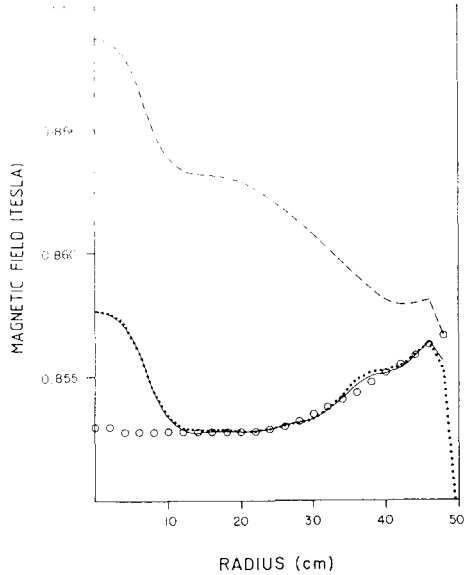

Fig. 9 Magnetic fields for 8 MeV protons: required average isochronous field (ooo), constructed average main field (---), constructed isochronous field (...) and measured average field (——).

is due to the fact that power supplies for the two cone coils were not available at the time of measurements.

6. Conclusion

The value of using computer programs for the calculation of 3-dimensional magnetic fields has clearly been demonstrated by the ease with which the magnet poles and sectors could be designed and the rapidity of the final shimming process, as well as by the excellent agreement obtained between the desired isochronous fields and the actual measured fields.

The program has saved us time and money by removing the need for model building, and also provided realistic fields for orbit calculations at a very early stage of the project.

During recent trials with the internal beam of the cyclotron, all coils were excited to theoretically calculated values. No apparent improvement in the beam current could be obtained by fine tuning of the main field, and we therefore conclude that the calculated current settings must be very close to the optimum values.

Acknowledgements

Mr.H.A. Smit was responsible for most of the mechanical design of the magnet, pole-gap coils and magnetic field measuring equipment. Dr. G.F. Burdzik and Mr. J.N.J. Truter were responsible for the computer control of the magnetic field measuring equipment.

References

1. H.N. Jungwirth and W.G. van der Merwe, IEEE Trans. Magn. (1983) 2611.

2. G.S.Z. Guasco, Private communication.

3. P.M. Cronje and G.S.Z. Guasco, NAC Internal Report IM/79-07.